Nanotoxicology, 2012; Early Online, 1–10

ISSN: 1743-5390 print / 1743-5404 online
DOI: 10.3109/17435390.2012.737484

informa
healthcare

Effects of particle size and coating on nanoscale Ag and TiO_2 exposure in zebrafish (*Danio rerio*) embryos

Olivia J. Osborne[1], Blair D. Johnston[1], Julian Moger[2], Mohammed Balousha[3], Jamie R. Lead[3], Tetsuhiro Kudoh[1] & Charles R. Tyler[1]

[1]*Biosciences, College of Life and Environmental Sciences, University of Exeter, Stocker Road, EX4 4QD, UK,* [2]*Physics, College of Engineering, Mathematics and Physical Sciences, University of Exeter, Stocker Road, Exeter, EX4 4QL, UK and* [3]*School of Geography, Earth and Environmental Sciences, University of Birmingham, Birmingham, UK*

Abstract

Manufactured metal (oxide) nanoparticles are entering the aquatic environment with little understanding on their potential health impacts for exposed organisms. Adopting an integrative approach, we investigated effects of particle size and coating on biological responses for two of the most commonly used metal (oxide) nanoscale particles, silver (Ag) and titanium dioxide (TiO_2) in zebrafish embryos. Titanium dioxide nanoparticles (nominally, 4 nm, 10 nm, 30 nm and 134 nm) had little or no toxicity on the endpoints measured. Ag both in nano form (10 nm and 35 nm) and its larger counterpart (600–1600 nm) induced dose-dependent lethality and morphological defects, occurring predominantly during gastrula stage. Of the silver material tested 10 nm nanoparticles appeared to be the most toxic. Coating Ag nanoparticles with citrate or fulvic acid decreased toxicity significantly. *In situ* hybridisation analysis identified the yolk syncytial layer (YSL) as a target tissue for Ag-nano toxicity where there was a significant induction of the heavy metal stress response gene, metallothionein 2 (Mt2) at sub-lethal exposures. Coherent Anti-stroke Raman Scattering (CARS) microscopy provided no evidence for silver particles crossing the chorionic membrane in exposed embryos. Collectively, our data suggest that silver ions play a major role in the toxicity of Ag nanoparticles.

Keywords: nanoparticle, ecotoxicology, *Danio rerio*, embryo, titanium dioxide, silver

Introduction

Nanoparticles are being introduced rapidly into the consumer market but there is still little understanding on their potential consequences for human and environmental health. Two of the first metal-based nanoparticles to gain widespread use are titanium dioxide (TiO_2) and silver (Ag). Titanium dioxide is of global importance with in excess of 4.3 million tonnes produced annually, with extensive use in sunscreen and in the pigmentation of paints. The surface reactivity and general properties of TiO_2 are well documented (Long et al. 2007). Nano-TiO_2 has been reported to cause oxidative stress effects in mammals and in fish, inducing inflammation, cell damage and genetic damage, both with and without exposure to ultraviolet A (UVA) radiation. Available data suggest sub-lethal toxicity in the concentration range of 5–50 μg L^{-1} for exposures through the water in both invertebrates (Lovern et al. 2007; Heinlaan et al. 2008; Zhao et al. 2009) and fish (Lee et al. 2007; Scown et al. 2009). Modelled environmental concentrations indicate TiO_2 concentrations may in some circumstances reach between 0.7 and 16 μg L^{-1} (Nowack & Bucheli 2007) and this could present a risk to aquatic organisms.

In the 1970s, 2.5 million kg of Ag was discharged into the environment in the United States (Luoma & Rainbow 2008) and its high toxicity to aquatic animals subsequently led to stringent environmental regulations by the 1980s under the Clean Water Act in the United States (Purcell & Peters 1999). Nano-silver is now used extensively in consumer products, predominantly for its effective antimicrobial properties and low production cost. In wastewater treatment works receiving influents from industries using silver nanoparticles (Ag NPs), levels of silver have been shown to reach 100 μg L^{-1} (Hu 2010), and this exceeds tolerable limits for some bacteria, which may therefore impact adversely on bacterial communities (Marambio-Jones & Hoek 2010). Of particular concern is the potential for nano-silver to concentrate in sewage sludge as in some countries (including the United Kingdom) this can be subsequently applied to land as fertilizer. Several studies have indicated that Ag NPs have the potential to induce toxic effects in a range of species, including fish (Skebo et al. 2007; Braydich-Stolle et al. 2005; Hussain et al. 2005; Scown et al. 2009; AshaRani et al. 2009). One study exposing zebrafish embryos to an extremely high level of Ag NPs (100 mg L^{-1}), that were stabilised

Correspondence: Tetsuhiro Kudoh and Charles R. Tyler, Biosciences, College of Life and Environmental Sciences, University of Exeter, Stocker Road, EX4 4QD, UK. E-mail: T.Kudoh@exeter.ac.uk and C.R.tyler@ex.ac.uk

(Received 14 May 2012; accepted 1 October 2012)

with citrate or fulvic acid, showed silver penetrated into various body tissues, including brain, heart and skin (AshaRani et al. 2009). This toxicity for exposure to Ag NPs in fish may, in part, relate to an enhanced dissociation in the exposure water, and thus bioavailability, of free silver ions (Jin et al. 2010).

The purpose of this study was to adopt an integrative approach to determine potential toxicity to zebrafish embryos of well-characterised Ag and TiO_2, of various sizes both as unmodified nanoparticles and dispersed with citrate or fulvic acid, and across a range of exposure concentrations. Zebrafish embryos offer a wide range of experimental conveniences including the ease for observing developmental effects through a transparent chorion. Mortality rates, developmental abnormalities, apoptosis and targeted (*in situ*) gene expression were used as effects assessment endpoints. Advanced imaging techniques, including Coherent Anti-strokes Raman Scattering (CARS) were employed to investigate for uptake and distribution of nanoparticles in the tissues of the exposed embryos.

Materials and methods

Fish source, culture and husbandry

Wild-type WIK (Wild-Type India Calcutta) strain zebrafish embryos were obtained from the Max Planck Institute, Tubingen, Germany, and maintained at University of Exeter as described in the supplementary material (S1).

Nanoparticle source and characterisation

Ag NPs (nominal sizes 10 nm and 35 nm) and Ag bulk (nominal size 600–1600 nm) were acquired from Nanostructured and Amorphous Materials Inc. Houston, USA. Titanium dioxide nanoparticles (TiO_2 NPs) (nominal sizes 3 nm, 10 nm and 35 nm) and 134 nm particles were acquired from Alfa Aesar- A Johnson Matthey Company, Lancashire, United Kingdom.

Physicochemical characterisation

A number of techniques were carried out to characterise and quantify the particles. The techniques applied included: nanoparticle tracking analysis (NTA), Braun Emmett Teller (BET) method of specific surface area analysis, X-ray diffraction (XRD), atomic force microscopy (AFM) and high-resolution transmission electron microscopy (HR-TEM) with associated spectroscopy – X-ray electron dispersive spectroscopy (X-EDS). A full detailing of the methods applied to Ag and TiO_2 particles can be found in (Scown et al. 2009); and details of data analysis in (Ju-Nam et al. 2012).

Silver dissolution

Samples of silver nitrate (Perkin Elmer) were made up in milli Q water and embryo culture water (0.60 mg of marine salts [Tropic Marin] per litre of deionised water) as test standards for analysis by the ICP-MS. Sample concentrations were 0, 15, 30, 60, 120 and 260 μg L^{-1}. Dissolution rates were determined for 35 nm silver and bulk silver particles. For this, duplicate 1 litre solutions containing 50 μg L^{-1} Ag NPs were made up in embryo culture water and mixed constantly using magnetic stirrers at a temperature of 21°C. For each treatment, 8 Spectra/por dialysis membranes MWCO 1000 (1 KDa) (prewashed in 0.05% sodium azide in Milli Q water) were set up containing 10 mL of Milli Q water, which were then clip sealed at each end before being submerged into the Ag NP or Ag bulk solutions. At different time points, 4 h, 24 h, 48 h and 72 h, one sample for each treatment vessel (two per treatment) was taken, pipetted into a 15 mL falcon tube and the silver ions stabilised through the addition of 1% of HNO_3 added before analyses using ICP-MS.

Ag/TiO_2 nanoparticle exposure and effects assessments

Particles were made up in a dilution series of six stock solutions (50 μg L^{-1}, 500 μg L^{-1}, 5000 μg L^{-1}, 50,000 μg L^{-1}, 250,000 μg L^{-1}) for each particle size. Solutions were sonicated in a water bath for 30 min and placed into glass, amber, Boston round 125 mL tubes fitted with a Teflon-lined cap and kept at 4°C until required. When the solutions were required for the exposure studies, they were sonicated in a water bath for 30 min and pipetted into the exposure wells. To investigate for effects of particle coating on biological effects a further dilution series of 10 nm Ag particles was mixed with either 0.0075% sodium citrate or a 2% fulvic acid suspension prior to the exposures. For the exposures to silver ions, a stock solution of silver nitrate (Perkin Elmer 2% $AgNO_3$) was made and the required amount for each exposure concentration was added into the embryo culture water.

For the embryos exposures, 500 μL of the stock solutions were added to 450 mL embryo culture medium to give final exposure concentrations of 5 μg L^{-1}, 50 μg L^{-1}, 500 μg L^{-1}, 5000 μg L^{-1} and 25,000 μg L^{-1}. Controls received 5 mL of embryo culture water only. Eggs/embryos were collected from breeding colonies transferred into a Petri dish and washed twice with embryo culture water with the addition of 15 μL of methylene blue to prevent fungal and bacteria growth. For all exposures, there were 20 embryos (at the 1–2 cell stage, 1–1.5 hpf) per treatment well, and the studies were replicated at least three times. The embryos were incubated at 28 +/– 1°C up to 48 h. After 2 h in culture, the numbers of unfertilised embryos were recorded and these were removed. At 48 hpf (hours post fertilisation) survival rates and any phenotypic deformities were recorded. Any physical deformities observed were recorded and converted to percentages for each treatment. Embryos were observed and photographed using Nikon SMZ1500 microscope equipped with a digital camera. To gain an insight into the timing of mortality and developmental effects induced by the exposures to Ag, time lapse video analysis was used, as described in the supplementary material (S2).

Cell necrosis

To investigate further for silver particle toxicity, cell necrosis was recorded in embryos exposed during early life to either 35 nm Ag or 35 nm TiO_2 at concentrations of 500 μg L^{-1} and 25,000 μg L^{-1}. Twenty embryos for each exposure concentration were incubated at 28 +/– 1°C from the 1 to 2-cell stage and subsequently removed from the exposure at 7 hpf and stained with a Propidium Iodide (PI) (Sigma) at 1 mg/mL

mixed in distilled water; Fluorescine Diacetate (DAF) (Sigma) at 1.5 mg/mL mixed in DMSO; Hoechst (HO) (Sigma) at 1 mg/mL mixed in distilled water and PBS (Pinero et al. 1997). The final concentrations of materials in the necrotic staining solution were PI, 250 mg L^{-1}; DAF, 750 μg L^{-1}; and HO, 200 μg L^{-1}. Embryos were incubated in the dark for 10 min in a 24-well plate and photographed using Leica DMI 4000 B Compound Microscope equipped with a digital camera.

Metallothionein gene expression assessed through whole mount *in-situ* hybridisation

In situ hybridisation on exposed zebrafish larvae was undertaken to investigate for differential activation of gene expression for metallothionein 2 (Mt2), known to play key roles in toxicological responses to metals, including silver (Choi et al. 2009). Mt2 cDNA was obtained from Imagene/RZPD (clone No IMAGp998C0115598Q). To prepare the RNA probe, Mt2 cDNA was amplified by PCR using two primers, Mt2_F: ATC AAC TCA TTC ACA AGC TGA; T3_Mt2_R: GGA TCC ATT AAC CCT CAC TAA AGG AAA TAC CAC CAT TTA TTT TAG, and *in vitro* transcribed by using digoxigenin labelling mixture (Roche) and T3 RNA polymerase (Promega). Using a G50 column the RNA was purified and precipitated using Lithium Chloride. The probe was then diluted with hybridisation buffer at 1/200. The *in situ* hybridisations were conducted as described in the supplementary material (S3). For these studies embryos were exposed to 35 nm Ag and 35 nm TiO_2 particles at 500 μg L^{-1} and Ag NO_3 at 12 μg L^{-1} (to represent the maximal rate of dissolution for the silver particle exposures – see results) from 1–2 cell stage to 24 hpf, fixed with 4% PFA (S3). Embryos were observed and photographed using Nikon SMZ1500 microscope equipped with a digital camera. The expression level for Mt2 expression (localised in the YSL) was quantified using Image-J 1.44 P. The levels of expression were determined from the mean of 15–20 embryos for each treatment subtracting for the background measurement. Responses to silver treatment were then given as fold-increase above controls.

CARS microscopy

To investigate the uptake of nanoparticles into the exposed embryos, Coherent Anti-Stokes Raman Scattering (CARS) microscopy was used to provide label-free imaging with sub-cellular resolution (S5). For this imaging work, embryos were exposed at the 1-cell stage to 500 μg L^{-1} and 5000 μg L^{-1} 35 nm Ag and 35 nm TiO_2 and their bulk counterparts. Ten embryos were taken at random for each exposure concentration at 24 hpf, five of which were manually dechorionated and the other five the chorion left intact. Embryos were embedded in 1% low melting agarose with 0.05% of tricaine (to anaesthetise the fish) in a glass-bottomed petri dish photographed using IX71 and FV300, Olympus, UK.

Statistics

Unless stated otherwise, all data are presented as means ± S.E.M. The coefficient of variation (CV) statistic was calculated for comparisons of variation, as CV = (standard deviation/mean)*100. All statistical analyses were performed using Sigma Stat version 12.0 (Jandel Scientific Software, USA). Differences among groups were analysed by one-way/two-way ANOVA, followed by Holm-Sidak method comparison post hoc test, where data were not normally distributed. All data were considered statistically significant at $p < 0.05$.

Results

Particle characterisation

A summary of the characterisation and physiochemical properties of the silver particles is provided in the supplementary material Table S4 and further details are reported elsewhere (in Scown et al. 2009). All particles had purity > 99% based on trace metal analysis. The measured sizes by TEM were found to be different from those reported by the manufacturer (the nominals) and were 49.0 ± 18.5 nm and 114.0 ± 65 nm for the 10 nm and 35 nm particles, respectively. In our assessments, 10 nm Ag particles had a specific surface area of 9–11 m^2 g^{-1}, bulk density of 2.05 g cm^{-3} and a true density of 10.5 g cm^{-3}. The 35 nm Ag particles had a density of 10.5 g cm^{-3}, a specific surface area of 30–50 m^2 g^{-1}, and a bulk density of 0.30–0.60 g cm^{-3}. Ag bulk particles had a range in particle size of 0.6–1.6 μm and purity of 99.95%.

The measured physicochemical properties of TiO_2 and TEM images of the different sized materials are shown in the supplementary material Table S1 and Figure S1, respectively. When in suspension, particles formed large aggregates of several hundreds of nanometres (Supplementary material Figure S1, Table S1). The high-resolution TEM micrographs show that both the 3 nm and 35 nm were comprised of very small particles likely to be less than 10 nm, but their precise dimensions were not resolved due to the dense aggregation resulting in the formation of sheet-like structures. The 10 nm particles formed fractal (i.e., porous) aggregates of about 19.1 ± 13.8 nm, as measured by TEM. It is worth noting the relatively high polydispersity of this sample (Supplementary material Figure 1B, inset). The TEM measurement for 10 nm particles were in good agreement with the sizes calculated from the SSA measured through the BET data and crystallite size measured by XRD (Supplementary material Table S1). The crystallite sizes were slightly larger than those measured by TEM or calculated from SSA, most likely due to the high polydispersity and aggregation observed. Measured sizes of the TiO_2 were thus again different from the data supplied by the manufacturer.

Dissolution of silver

Mean recoveries of silver for the silver nitrate control standards (in Milli Q water) were between 78% and 103%, with greater recoveries at the higher concentrations (Supplementary material Table S2). In contrast, quantification of silver in embryo culture water gave measured concentrations between 9.9% and 64.2% of nominals (Supplementary material Table S3). Dissolution of silver ions over the 72 h period for 50 μg Ag NP L^{-1}, ranged between 0.1% and 2%, and for 50 μg Ag bulk L^{-1} between 0.21% and 0.83%.

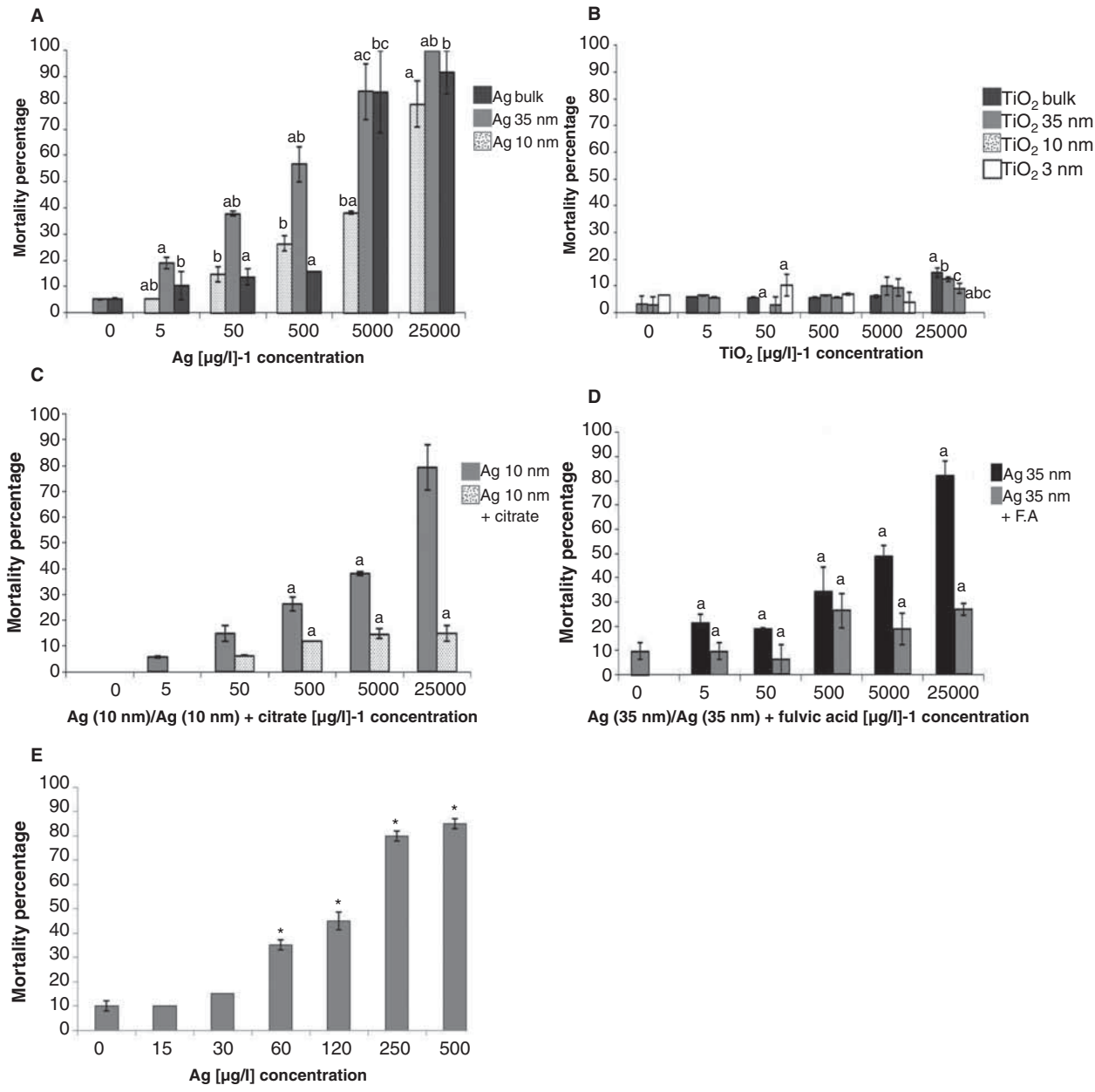

Figure 1. Mortality and morphological abnormalities at 48 hpf in zebrafish embryos exposed to Ag nanoparticles (nominal sizes), TiO_2 nanoparticles (nominal sizes), Ag coated with citrate, Ag coated with fulvic and AgN03. Mortality rates are shown for exposure to silver particles (A), TiO_2 particles (B), Ag (10 nm) and Ag (10 nm) citrate-coated particles (C), Ag (35 nm) and Ag (35 nm) with fulvic acid (D), silver nitrate (E). For the different exposures there were statistically significant interactions between concentration and particle size (A, B, E), citrate coating (C) or fulvic acid (D) (Two-way ANOVAs $p < 0.001$). The letters (a, b, c) indicate statistical difference ($p < 0.05$) between particles/coating for each concentration tested (All Pairwise Multiple Comparison Procedures, Holm-Sidak method). There was no statistically significant interaction between concentration and particle size for effects on heartbeat rate (Two-way ANOVA $p = 0.817$). Significant differences in mortality between the treatment groups for exposure to silver nitrate were assessed by One-way ANOVA (*$p < 0.0001$) to that of the control group.

Lethality

Overall TiO_2 had an extremely low level of toxicity: 3 nm and 35 nm TiO_2 particles showed no toxicity and the lowest effect concentration for 10 nm TiO_2 was 5000 µg L^{-1} ($p = 0.029$) and for 134 nm TiO_2, 25,000 µg L^{-1} ($p = 0.004$; Figure 1B). In contrast, there was a clear dose-dependent toxicity for the different sized Ag NPs and the bulk counterpart (Figure 1A). There was a statistically significant interaction between concentration and Ag particle size (Two-way ANOVA $p < 0.001$) with the following lowest effect concentrations: 5 µg L^{-1} for 35 nm Ag ($p = 0.002$), 50 µg L^{-1} for both 10 nm Ag ($p < 0.001$) and Ag bulk ($p = 0.003$). The 35 nm Ag was significantly more toxic than 10 nm Ag across all concentrations and it was also significantly more toxic than Ag bulk for almost all concentrations tested (the exception was for 5 µg L^{-1}). Exposure to silver ions showed a dose-dependent toxicity with a no effect concentration (NOEC) of 30 µg L^{-1} and a lowest effect concentration (LOEC) of 60 µg L^{-1} ($p < 0.001$, Two-way ANOVA). At 500 µg L^{-1} there was 85% embryo mortality (Figure 1E).

Effects of coating on silver nanoparticle toxicity

Coating the 10 nm Ag with citrate significantly reduced their toxicity across the concentration range tested

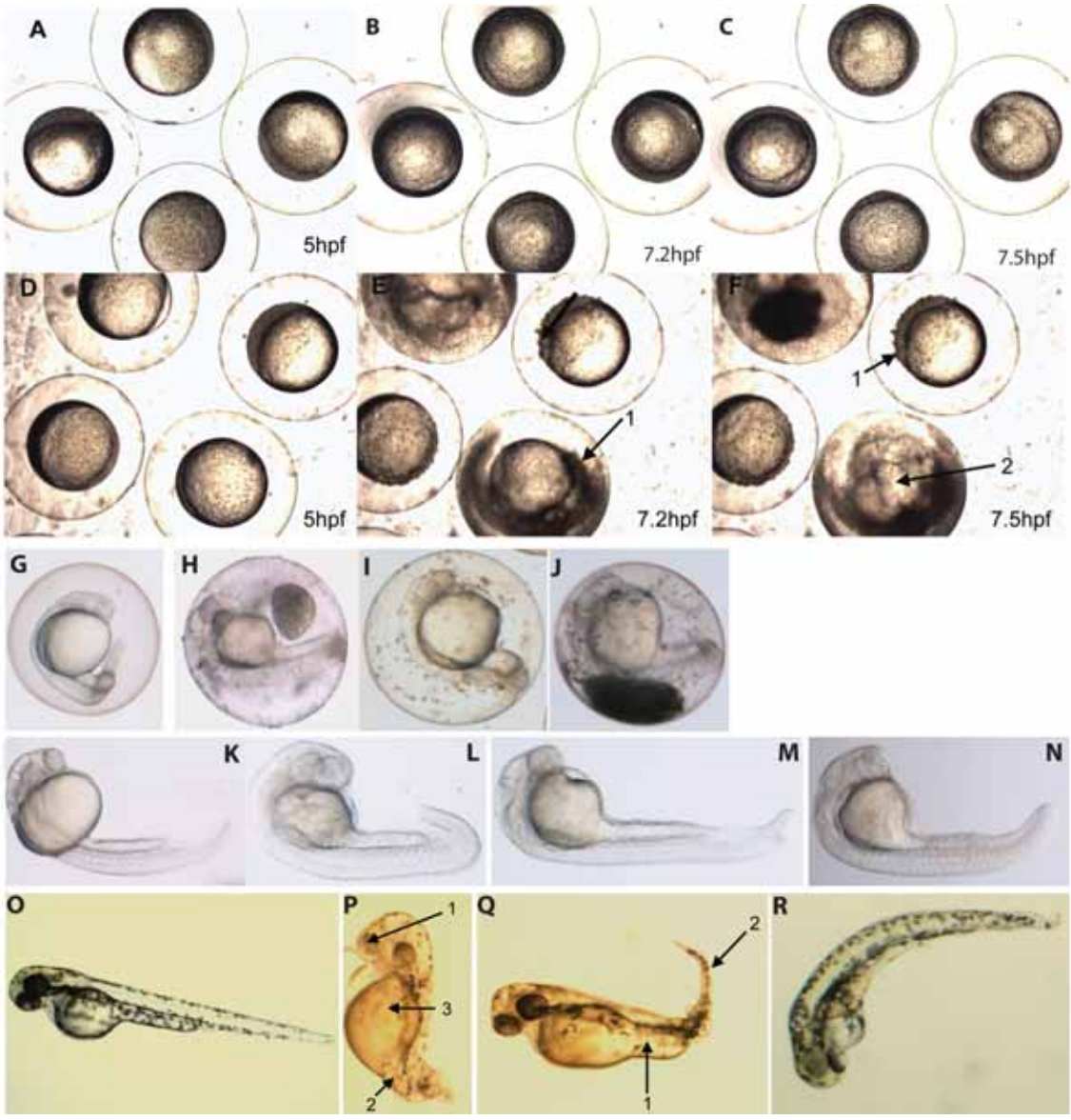

Figure 2. Images of embryos exposed to silver particles at various developmental stages. Video-captured images of zebrafish embryos in controls (A-C, 5 hpf, 7.2 hpf and 7.5 hpf, respectively) and exposed to silver particles (35 nm Ag at 25,000 μg/L) from 1–2 cell stage (D-F, 5 hpf, 7.2 hpf showing – 1.Yolk leaking out from the cells, 7.5 hpf showing – 1. Uneven surface of dividing cells, 2. Embryo bursting within the chorion membrane). G-R, microscope images of control/exposed embryos at different developmental stages. G. 24 hpf control embryo; H.24 hpf Ag (10 nm 5000 μg/L); I. 24 hpf Ag (Bulk 5000 μg/L); J. 24 hpf $AgNO_3$ (120 μg/L); K. 24 hpf control embryo; L. 24 hpf Ag (35 nm 500 μg/L); M. 24 hpf Ag (Bulk 500 μg/L); N. $AgNO_3$ (120 μg/L); O. 48 hpf control embryo; P. 48 hpf Ag (35 nm, 5000 μg/L), showing – 1. Eyes spaced more widely on the head compared with controls, 2. absence of a tail and 3. deformed yolk sac; Q. 24 hpf Ag (Bulk, 5000 μg/L) showing – 1.bent tail, 2. reduced yolk sac; R. $AgNO_3$ (120 μg/L).

(Two-way ANOVA $p < 0.001$) (Figure 1C). The maximum mortality rate (exposure to 25,000 μg L^{-1}) in the citrate-coated silver particles was 14% compared with 79% for non-coated silver particles of the same size. The lowest effect concentration for 10 nm Ag was 50 μg L^{-1} ($p < 0.001$) and for Ag 10 nm + citrate, 500 μg L^{-1} ($p = 0.05$, Two-way ANOVA). The 10 nm Ag was more toxic than 10 nm Ag coated with citrate for all concentrations above 50 μg L^{-1}.

Similarly, the addition of fulvic acid significantly reduced the toxicity of the 35 nm Ag (Two-way ANOVA $p < 0.001$) (Figure 1D). The lowest effect concentration for 35 nm Ag was 5 μg L^{-1} ($p < 0.001$) and for 35 nm Ag with fulvic acid, 500 μg L^{-1} ($p < 0.001$). The 35 nm Ag was significantly more toxic than 35 nm Ag + fulvic acid for all adopted exposure concentrations.

Ag-nano predominantly induces embryonic lethality at gastrula stage

Video analysis on the developing embryos in the controls established that at 8 hpf half had reached gastrulation stage, which is in accordance with the normal progression of expected development. In contrast, half of the embryos exposed to 25,000 μg Ag L^{-1} had died by this stage. Time lapse analysis showed that for embryos exposed to 35 nm Ag the yolk sac membrane of the embryo became damaged, leading to the leakage of yolk and subsequently mortality (Figure 2). It was observed that the surface of the blastoderm

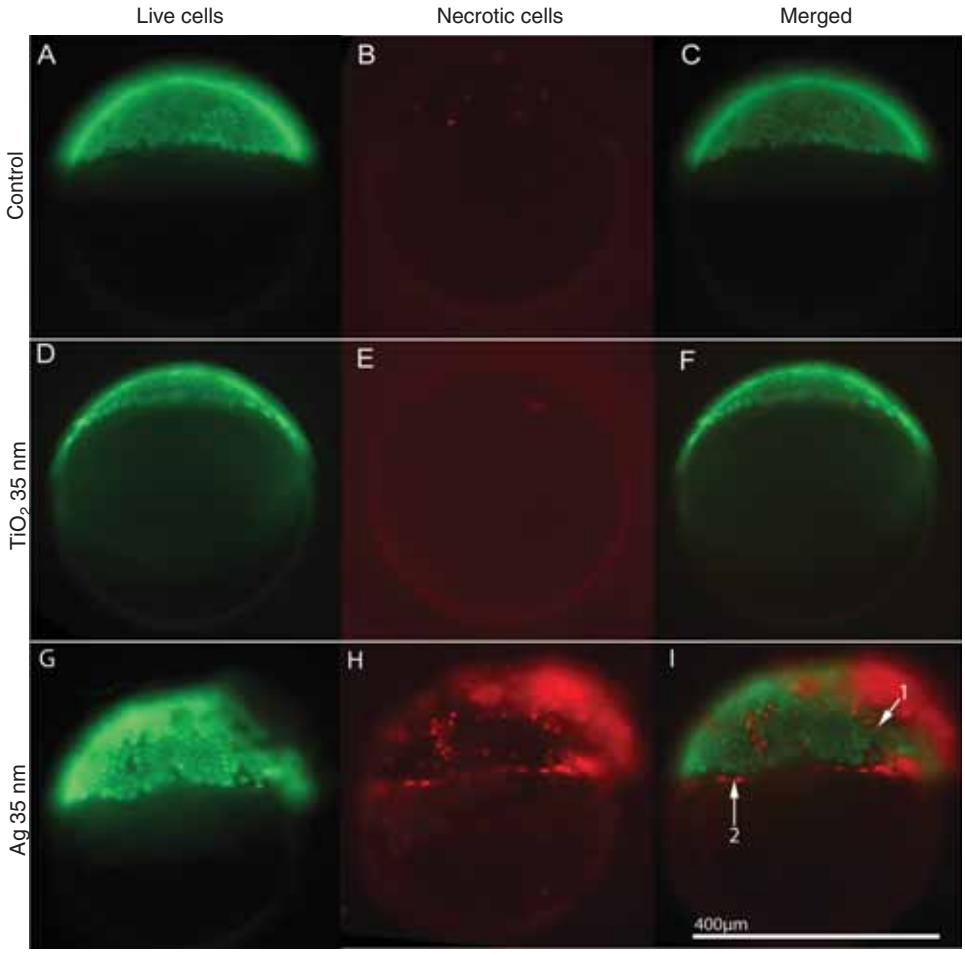

Figure 3. Images showing live (green)/necrotic (red) cells in embryos at shield stage (Lateral View). A. control-live cells; B. control-necrotic cells; C. control-merged images live/necrotic cells; D. TiO_2 (35 nm 500 µg/L) – live cells; E. TiO_2 (35 nm 500 µg/L) – necrotic cells; F. TiO_2 (35 nm 500 µg/L) – merged live/necrotic cells; G. Ag (35 nm 500 µg/L) – live cells; H. Ag (35 nm 500 µg/L) – necrotic cells; I. Ag (35 nm 500 µg/L) – merged live/necrotic cells, showing – 1. necrotic nuclei in blastoderm, 2. necrotic nuclei in yolk syncytial layer (YSL).

became rough (Figure 2E, F) and epiboly, the process where cells move and spread out into sheets of tissue that overlie or surround other groups of cells, was delayed in comparison with control embryos (normally occurring at approximately 4 hpf). The blastoderm in the surviving embryos treated with 35 nm Ag did not cover the yolk and had only reached approximately 40% epiboly in comparison with the control embryos where there was nearly 70% epiboly. Embryos that survived the exposure to silver at high exposure concentrations subsequently had morphological abnormalities including bent tails, small head and a reduced yolk sac size (Figure 2G–R).

Cell necrosis in early life stage embryos

Staining for cell necrosis during the gastrula stage (7 hpf) identified a high prevalence cell death in the exposures to 35 nm Ag (500 µg L^{-1} and 25,000 µg L^{-1}; Figure 3H, I). In the controls and embryos exposed to TiO_2 there was a very low/no incidence of necrotic cells (Figure 3B, E). Based on a qualitative assessment only, there appeared to be similar numbers of live cells in all embryos examined in controls, TiO_2 exposures and for Ag at 500 µg L^{-1} (Figure 3A, D, G). There was a high level of necrotic nuclei in the yolk syncytial layer (YSL) (Figure 3I).

Particle uptake (CARS)

The studies showing cell damage for the high concentration exposures suggested that material (particles and/or free silver) entered the embryo from the culture medium. CARS microscopy, however, showed no detectable particles contained within the exposed embryos (Figure 4). CARS images, including images that were focused at the outside edge of the chorion (Figure 4B, C), for exposures of embryos to both Ag NPs and TiO_2 NPs, illustrate that the particles were associated with the outer edge of the embryo and not contained with the embryo itself.

Expression of metallothionein

We conducted *in situ* hybridisation with Mt2 to identify possible tissue targets for metal responses induced by exposure to Ag-nano. For the exposures to all silver-treatment groups at sub-lethal doses, and for which no significant morphological defects were found, significant induction of Mt2 was detected in the YSL especially at the posterior extension. Exposure to 35 nm Ag (Figure 5C, E) induced a 3.9-fold increase, Ag bulk material induced a 2.7-fold increase (Figure 5B, E) and Ag ion (12 µg L^{-1}) induced a 2.8-fold increase (Figure 5D, E). TiO_2 (500 µg L^{-1}) did not show any enhanced expression of Mt2.

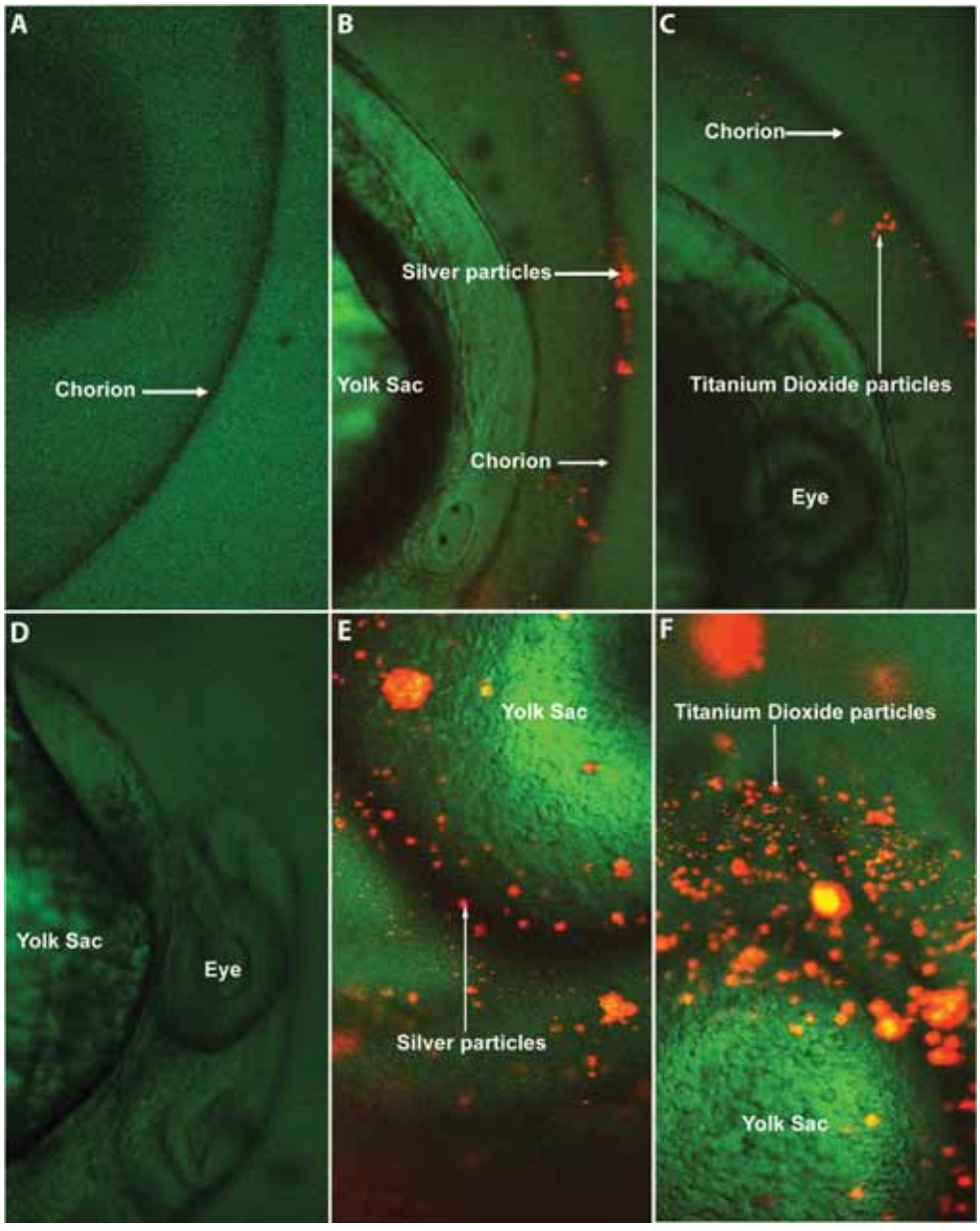

Figure 4. Coherent Anti-stokes Raman Scattering images of embryos exposed to silver and titanium nanoparticles after 24 h. Aggregates of nanoparticles appear as coloured (yellow/red) patches on the image. NPs were visible only on the outside of chorion membrane. A. Control embryo – showing chorion margin; B. Embryo exposed to Ag (35 nm, 25,000 μg/L) – showing chorion margin; C. Embryo exposed to TiO_2 (35 nm, 25,000 μg/L) – showing chorion margin; D. Control embryo showing chorion surface of embryo; E. Embryo exposed to Ag (35 nm, 500 μg/L) showing silver particles on chorion surface of embryo; F. Embryo exposed to TiO_2 (35 nm, 500 μg/L) showing titanium dioxide particles on chorion surface of embryo. CARS revealed nanomaterial on the surface of the chorion, likely as aggregates of nanoparticles B, C, but none were detected internally to the chorion within the embryo itself.

Discussion

We found TiO_2 nanoparticles had little or no toxicity in zebrafish embryos on the endpoints measured and at exposure levels far exceeding those predicted to occur in some of the most polluted environments (Colvin 2003). Our data support the majority of previous studies in this regard and would suggest, therefore, that in natural environments exposure to the TiO_2 particles tested are unlikely to pose any obvious health threat to fish embryos, which are widely accepted as highly sensitive to the effects of a wide range of toxicants.

In contrast Ag induced a dose-dependent toxicity in both nano and bulk form. One possible explanation for the enhanced toxicity of the Ag-nano is that the particles themselves may interfere with biological processes because they have the potential to by-pass barriers which normally prevent larger molecules from entering (Scown et al. 2010). It is thought that nanoparticles can enter through pathways such as tight junctions (Luhmann et al. 2008) and, if this is the case, in turn block the channel pathways of epithelial membranes (Hunziker et al. 2009). But for these particles, this is unlikely as they were aggregated. Furthermore, an enhanced ability to cross cell membranes was not supported by the CARS imaging in this study, where at 24 hpf we found no evidence for uptake of Ag (or TiO_2) nanoparticles into the embryo (Figure 4).

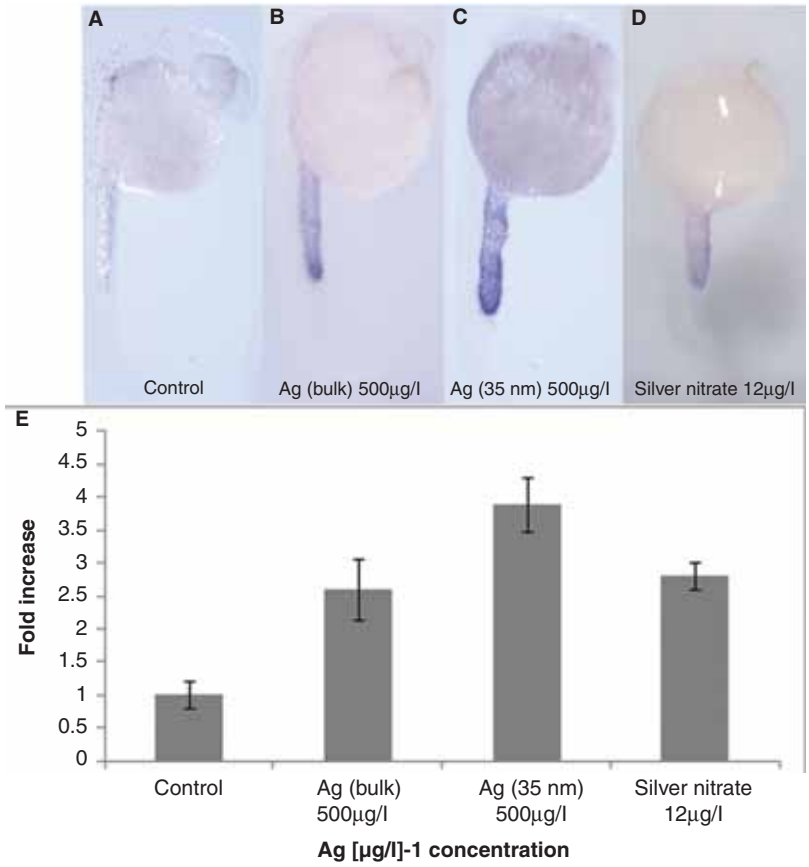

Figure 5. Embryos (24 hpf) after applying the technique *in situ* hybridisation to investigate the expression of metallothionein 2 as a measure of metal exposure/toxicity. There was a very low expression signal in the YSL especially at the posterior extension in the control embryos and in the embryos exposed to TiO_2, but high expression in the Ag nano/bulk exposed embryos. A. Control embryo, B. Embryo exposed to Ag (Bulk 500 µg/L), C. Embryo exposed to Ag (35 nm, 500 µg/L), D. Embryo exposed to $AgNO_3$ (12 µg/L), E. Graphical representation of the fold-increase Mt2 expression in the different treatments.

Time lapse video analysis of the embryos exposed to nano and bulk silver established that it was during gastrulation, when the yolk sac folds in on itself over the cells, when the greatest mortality occurred. The necrosis assay confirmed a high incidence of damaged nuclei both in the blastoderm and the YSL in the Ag-exposed embryos at this development period (7 hpf). We recently reported that deformity of the YSL often results in failure of gastrulation cell movement which leads to embryonic lethality at the gastrula stage (Takesono et al. 2012) The developmental morphologies seen for exposure to silver particles (i.e., bent tails and a small head) are common for embryos exposed to xenobiotic compounds (Yeo & Kang 2008) and some abnormalities likely result from failed epiboly movement.

Citrate is used widely to stabilise NPs to prevent/reduce their aggregation (Baveye & Laba 2008), and here we found that coating 35 nm Ag particles with citrate reduced significantly rates of mortality and abnormalities in exposed embryos compared with uncoated 35 nm Ag; the LC50 of 35 nm Ag was 500 µg L^{-1} compared with 5000 µg L^{-1} for 35 nm Ag coated with citrate (i.e., 10-fold lower). No studies were undertaken to investigate the aggregation behaviour of the different particles in the embryo incubation water, but some other studies have shown that in high ionic strength water there can be an enhanced aggregation rate for particles coated with citrate (Christian et al. 2008). It is possible therefore that an enhanced aggregation of the citrate-coated particles resulted in a lower bioavailability of silver particles/ions for uptake. Subtle differences in the nature of nanoparticle have also been found to profoundly affect biological effects responses (Moore 2006). An alternative hypothesis is that the toxicity of the silver nanoparticles derives from the dissolution of silver ions from the particles, and the rate of this process is much reduced in citrate-coated silver particles (Treuel et al. 2010; Studer et al. 2010; Kittler et al. 2010). Similarly, addition of fulvics to the medium also reduced the toxicity of the silver nanoparticles to the fish embryos. Such a coating could affect the particles by reducing silver particle dissolution rates, and/or complexing free Ag ions after dissolution.

It is well established that fish and many other aquatic animals are sensitive to the toxic effects of silver ions, with LC10 concentrations reported for rainbow trout (*Oncorhynchus mykiss*) between 0.7 µg L^{-1} and 0.8 µg L^{-1} and LC50 between 10 µg L^{-1} and 240 µg L^{-1} for freshwater fish species (Birge & Zulderveen 1996). The degree of dissolution (up to 2%) we found for Ag 35 nm equates well with previous literature (Kittler et al. 2010; Fabrega et al. 2009). Based on the amount of silver ions in solution, it appears that they do not explain all of the toxicity observed. However; the silver particles settle on the embryo surface (as evidenced by the CARS imaging), and therefore the local concentration of

dissolved Ag ions is likely to be higher at the membrane surface compared with the surrounding medium and therefore may explain all toxicity observed in our experiments. Nevertheless, it is still possible that the NP is having an effect directly on toxicity. These discrepancies further highlight the need for stringent reporting on the physiochemical characterisation of materials used. A further difficulty in relating the toxicity effects with the measured Ag^+ is that the embryo medium contained relatively high levels of chloride ion (626.2 μmol L^{-1}), and this can complex Ag^+ and in turn reduce its toxicity.

CARS images (Figure 4) illustrated that the nanomaterials, generally appearing as aggregates, were associated with the outer edge of the embryo (panels B and C) with no evidence for penetration of the embryo itself. This was supported by CARS images of embryos that were dechorionated and showed an absence of any nanomaterial at the embryo surface and again no evidence of body penetration. Contrasting with this, however, expression of Mt2, that plays a central role in metal transport, storage and detoxification (Ngu & Stillman 2006), strongly supports an intracellular presence of silver ions in exposed embryos/larvae.

We identified Mt2 expression in the (YSL) of the embryo, a body region where processing of xenobiotic compounds is known to occur in zebrafish embryos (Chen et al. 2004). The YSL was both the target for a toxicology response (cell necrosis) to Ag nanoparticles at the gastrula stage of development and location of Mt2 expression later in development (24 hpf), for exposure to the lower Ag exposure concentration. We found low level and more diffuse expression of Mt2 at 7.2 hpf compared with at 24 hpf, and this may confer a lower resistance of earlier life stage embryos to the toxic effects of Ag, but this would need further investigation to confirm this hypothesis. No such gene upregulation was seen in TiO_2-exposed embryos. These findings provide further evidence that at least some of the Ag toxicity relates to the bioavailability of silver ions that may be more readily released from nanoform silver. This would indicate the possibility for greater health effects associated with silver for Ag nanoparticle exposure. Our data further show Mt2 as an effective biomarker for exposure to silver nanoparticles in fish embryos. Where the release of silver ions occurs to induce the response in Mt2 is not known, it may potentially occur outside of the embryo from where the silver ions are then transported into the embryo or be released from Ag NPs that have penetrated the embryo, or a combination of both.

Conclusion

Our findings indicate that TiO_2 nanoparticles are not likely to have adverse biological effects in fish in the natural environment. In contrast, Ag NPs at sub-lethal exposure concentrations have the potential to induce harmful effects, disrupting embryo development predominantly at gastrula stage, inducing embryonic deformity at 1–2 cell stage and inducing the heavy metal stress response gene Mt2 in the (YSL). These reported effects occur predominantly at exposure levels exceeding those currently found (or estimated) in the most aquatic environments but with the rapid expansion in the use and discharge of Ag NPs, concentrations in the aquatic environment are likely to rise in the near future (Simonet & Valcárcel 2009); reviewed in (Fabrega et al. 2011) heightening potential health concerns. Collectively, our data would suggest that silver ions play a major role in the toxicity of Ag NPs and furthermore we show that coating of the particles, here with citrate or natural organic matter (here fulvics) can reduce significantly associated toxicity with major implications for understanding toxicity of metal NPs in the natural environment.

Supportive Information

The supportive information contains extra information on the materials and methods. In addition it contains data for the characterisation of the titanium dioxide particles.

Acknowledgements

The NERC funded Facility for Environmental Nanoscience Analysis and Characterisation (FENAC) is acknowledged for their support in generating the characterisation data.

Declaration of interest

This work was supported by the UK Environment Agency and NERC (NE/H013172/1) on grants to CRT.

References

AshaRani PV, Hande MP, Valiyaveettil S. 2009. Anti-proliferative activity of silver nanoparticles. BMC Cell Biol 10:65.

Baveye P, Laba M. 2008. Aggregation and toxicology of titanium dioxide nanoparticles. Environ Health Perspect 116:A152.

Birge W, Zulderveen J. 1996. The Comparative Toxicity of Silver to Aquatic Biota. University of Wisconsin System, Sea Grant Institute. Available at http://images.library.wisc.edu/EcoNatRes/EFacs/Argentum/Argentumv03/reference/econatres.argentumv03.birgetoxicity.pdf.Accessed October 2011.

Braydich-Stolle L, Hussain S, Schlager J, Hofmann M. 2005. In vitro cytotoxicity of nanoparticles in mammalian germline stem cells. Toxicol Sci 88:412.

Chen W, John J, Lin C, Lin H, Wu S, Chang C. 2004. Expression of metallothionein gene during embryonic and early larval development in zebrafish. Aquat Toxicol 69:215–227.

Choi JE, Kim S, Ahn JH, Youn P, Kang JS, Park K, et al. 2009. Induction of oxidative stress and apoptosis by silver nanoparticles in the liver of adult zebrafish. Aquat Toxicol 100:151–159.

Christian P, Von der Kammer F, Baalousha M, Hofmann T. 2008. Nanoparticles: structure, properties, preparation and behaviour in environmental media. Ecotoxicology 17:326–343.

Colvin VL. 2003. The potential environmental impact of engineered nanomaterials. Nat Biotechnol 21:1166–1170.

Fabrega J, Fawcett SR, Renshaw JC, Lead JR. 2009. Silver nanoparticle impact on bacterial growth: effect of pH, concentration, and organic matter. Environ Sci Technol 43:7285–7290.

Fabrega J, Luoma SN, Tyler CR, Galloway TS, Lead JR. 2011. Silver nanoparticles: behaviour and effects in the aquatic environment. Environ Int 37:517–531.

Heinlaan M, Ivask A, Blinova I, Dubourguier HC, Kahru A. 2008. Toxicity of nanosized and bulk ZnO, CuO and TiO2 to bacteria vibrio fischeri and crustaceans daphnia magna and thamnocephalus platyurus. Chemosphere 71:1308–1316.

Hu Z. 2010. Impact of Silver Nanoparticles on Wastewater Treatment. Water Intelligence Online 9:58. Available at http://www.mendeley.com/research/impact-silver-nanoparticles-wastewater-treatment/. Accessed November 2011.

Hunziker W, Kiener T, Xu J. 2009. Vertebrate animal models unravel physiological roles for zonula occludens tight junction adaptor proteins. Ann N Y Acad Sci 1165:28–33.

Hussain S, Hess K, Gearhart J, Geiss K, Schlager J. 2005. In vitro toxicity of nanoparticles in BRL 3A rat liver cells. Toxicol In Vitro 19:975–983.
Jin X, Li M, Wang J, Marambio-Jones C, Peng F, Huang X, et al. 2010. High-throughput screening of silver nanoparticle stability and bacterial inactivation in aquatic media: influence of specific ions. Environ Sci Technol 44:7321–7328.
Ju-Nam Y, Baalousha M, Cole P, Tyler C, Stone V, Fernandes T, et al. 2012. Characterisation of cerium dioxide NPs. Part I: size measurements. Environ Toxicol Chem in press.
Kittler S, Greulich C, Diendorf J, Kolller M, Epple M. 2010. Toxicity of silver nanoparticles increases during storage because of slow dissolution under release of silver ions. Chem Mater 22:4548–4554.
Lee KJ, Nallathamby PD, Browning LM, Osgood CJ, Xu XHN. 2007. In vivo imaging of transport and biocompatibility of single silver nanoparticles in early development of zebrafish embryos. ACS Nano 1:133–143.
Long T, Tajuba J, Sama P, Saleh N, Swartz C, Parker J, et al. 2007. Nanosize titanium dioxide stimulates reactive oxygen species in brain microglia and damages neurons in vitro. Environ Health Perspect 115:1631.
Lovern SB, Strickler JR, Klaper R. 2007. Behavioral and physiological changes in Daphnia magna when exposed to nanoparticle suspensions (titanium dioxide, nano-C60, and C60HxC70Hx). Environ Sci Technol 41:4465–4470.
Luhmann C, Chun M, Yi D, Lee D, Wang X. 2008. Neural dissociation of delay and uncertainty in intertemporal choice. J Neurosci 28:14459.
Luoma SN, Rainbow P. 2008. Metal contamination in aquatic environments: science and lateral management. Cambridge: Cambridge University Press.
Marambio-Jones C, Hoek EMV. 2010. A review of the antibacterial effects of silver nanomaterials and potential implications for human health and the environment. J Nanopart Res 12:1531–1551.
Moore M. 2006. Do nanoparticles present ecotoxicological risks for the health of the aquatic environment? Environ Int 32:967–976.
Ngu T, Stillman M. 2006. Arsenic binding to human metallothionein. J Am Chem Soc 128:12473–12483.
Nowack B, Bucheli TD. 2007. Occurrence, behavior and effects of nanoparticles in the environment. Environ Pollut 150:5–22.
Pinero J, Lopez-Baena M, Ortiz T, Cortes F. 1997. Apoptotic and necrotic cell death are both induced by electroporation in HL60 human promyeloid leukaemia cells. Apoptosis 2:330–336.
Purcell TW, Peters JJ. 1999. Historical impacts of environmental regulation of silver. Environ Toxicol Chem 18:3–8.
Scown T, Van Aerle R, Johnston B, Cumberland S, Lead J, Owen R, et al. 2009. High doses of intravenously administered titanium dioxide nanoparticles accumulate in the kidneys of rainbow trout but with no observable impairment of renal function. Toxicol Sci 109:372.
Scown T, Van Aerle R, Tyler C. 2010. Review: do engineered nanoparticles pose a significant threat to the aquatic environment? Crit Rev Toxicol 40:653–670.
Simonet B, Valcárcel M. 2009. Monitoring nanoparticles in the environment. Anal Bioanal Chem 393:17–21.
Skebo J, Grabinski C, Schrand A, Schlager J, Hussain S. 2007. Assessment of metal nanoparticle agglomeration, uptake, and interaction using high-illuminating system. Int J Toxicol 26:135.
Studer AM, Limbach LK, Van Duc L, Krumeich F, Athanassiou EK, Gerber LC, et al. 2010. Nanoparticle cytotoxicity depends on intracellular solubility: Comparison of stabilized copper metal and degradable copper oxide nanoparticles. Toxicol Lett 197:169–174.
Takesono A, Moger J, Farooq S, Cartwright E, Dawid IB, Wilson SW, et al. 2012. Solute carrier family 3 member 2 (Slc3a2) controls yolk syncytial layer (YSL) formation by regulating microtubule networks in the zebrafish embryo. Proc Natl Acad Sci 109:3371–3376.
Treuel L, Malissek M, Gebauer J, Zellner R. 2010. The influence of surface composition of nanoparticles on their interactions with serum albumin. ChemPhysChem 11:3093–3099.
Yeo M, Kang M. 2008. Effects of nanometer sized silver materials on biological toxicity during zebrafish embryogenesis. Bull Korean Chem Soc 29:1179–1184.
Zhao J, Bowman L, Zhang X, Vallyathan V, Young S, Castranova V, et al. 2009. Titanium dioxide (TiO 2) nanoparticles induce JB6 cell apoptosis through activation of the caspase-8/Bid and mitochondrial pathways. J Toxicol Environment Health A 72:1141–1149.

Supplementary material available online

Supplementary Tables SI–SIV.
Supplementary Figures S1, S2.